ADVANCED FUNCTIONAL MATERIALS
www.afm-journal.de

Modeling the Photoinduced Reconfiguration and Directed Motion of Polymer Gels

*Olga Kuksenok and Anna C. Balazs**

A remarkable feature of certain biological species is their ability to dramatically alter their shape in response to environmental cues. Here, a computational model for photoresponsive polymer gels that contain spirobenzopyran (SP) chromophores is developed, and it is shown that these materials can undergo 3D biomimetic shape changes under non-uniform illumination. The SP moieties are hydrophilic in the dark, but become hydrophobic under illumination with blue light. Hence, with the incorporation of these chromophores into gels in aqueous solutions, light can be harnessed to control the gel's swelling or shrinking and, thereby, dynamically alter the gel's shape. The model is first validated by determining the effects of uniform illumination on the temperature-induced volume phase transitions in these gels, and show good agreement between these results and available experimental data. These gels can also be patterned remotely and reversibly by illuminating the samples through photomasks and, thus, molded into a variety of shapes with feature sizes on the submillimeter length scale. Furthermore, by repeatedly rastering the light source over the sample, the system can be driven to exhibit another biomimetic behavior: sustained, directed motion. The introduction of a temperature gradient provides a means of further controlling this autonomous movement. The results point to a robust method for controllably reconfiguring the morphology of soft materials and driving the self-organization of multiple reconfigurable pieces into complex architectures.

1. Introduction

The ability to dynamically change shape in response to variations in the environment is a distinctly biological trait.[1,2] Through the environmentally driven shape-shifting, many biological species achieve one of their vital functions: survival.[1,2] The ability to undergo dynamic reconfiguration in response to external stimuli would prove particularly advantageous in the realm of functional materials. Namely, it would be highly desirable to create materials that could be molded via an external cue into a particular shape, which would permit a particular function. And then to use that same external cue to dynamically remold the given sample into another shape, which could enable a different function. Such processes would have a dramatic effect on manufacturing and sustainability since the same sample could be used and re-used for multiple applications, or multiple "lives". Inspired by the adaptability of shape-changing biological species, we use computational modeling to show that a soft, responsive material can be driven to undergo controlled variations in shape through the use of visual light.

Significant progress has been made in understanding shape changes in gel-based materials that encompass gradients in their properties,[3–6] and in designing shape-memory polymers that change their shape upon application of external stimuli.[7–9] In the latter systems, however, the shapes of the materials are typically pre-programmed during their fabrication. Here, we develop a computational approach to model polymer gels whose shapes can be reconfigured "on demand" through an application of non-uniform illumination. In addition, our simulations show that by repeatedly sweeping a light source over the material, the sample can be driven to exhibit another distinctive biological behavior: directed, sustained motion. To the best of our knowledge, this is the first example of a material that can undergo both multiple shape reconfigurations and directed motion in response to non-uniform illumination with visual light; the shape-changing and the directionality of the sample's movement are prescribed dynamically and no pre-programming is required to achieve these behaviors. Removing the light source results in the complete recovery of the material's initial shape and arrests the sample's net motion. The findings described herein can help guide new experimental studies to uncover the novel behavior predicted from these simulation studies.

To achieve the bio-inspired behavior described above, we focus on photosensitive polymer gels containing spirobenzopyran chromophores, which are anchored onto the polymers in the network.[10–12] Spiropyrans are a class of photochromic compounds that find widespread use in the fabrication of responsive polymeric materials.[13] In the absence of light and within acidic aqueous solutions, the spirobenzopyran chromophores are primarily in the open ring form (protonated merocyanine

Prof. O. Kuksenok, Prof. A. C. Balazs
Chemical Engineering Department
University of Pittsburgh
Pittsburgh, PA, 15261, USA
E-mail: balazs@pitt.edu

DOI: 10.1002/adfm.201203876

form, or *McH*) and are hydrophilic.[10,11,14] Illumination with blue light causes isomerization of these chromophores into the closed ring conformation (into the spiro form, or *SP*), which is hydrophobic. The incorporation of these chromophores into gels formed from N-isopropylacrylamide (PNIPAAm) in aqueous solutions provides a means of harnessing light to control the gel's swelling or shrinking.[10,11]

Researchers have exploited the photo-sensitivity of these *SP*-containing PNIPAAm gels to create films with rewritable micro-relief patterns that encompass well-defined features, which are tenths of microns in size[10] and demonstrated that such films can be used as a micro-conveyer to propel non-reactive glass beads along the substrate.[11] Researches also demonstrated the light-induced bending of rod-like *SP*-containing gels[11] and harnessed these gels as photo-controlled microvalves in microfluidic devices.[15] In the above systems, the *SP*-containing gels were constrained or bounded by hard surfaces; for example, the thin gel layer described in ref.[10] was covalently attached to an underlying glass plate.

Here, we primarily focus on *SP*-containing gels that are freely suspended within the solution. Hence, we can harness non-uniform illumination to configure these gels into a variety of complex, three-dimensional shapes, which can be dynamically altered by varying the pattern of illumination. While the dynamics of this reconfiguration exhibits a number of features that are similar to the shape changes driven by external stimuli in shape memory materials[7–9] or in various gel-based gradient materials,[3–6] the shape changes considered here only require the application of non-uniform illumination. Moreover, since the gels are either unattached or only partially attached to a surface, we can utilize the light to direct the net motion of the sample in a specified direction.

Notably, when the light is removed, the *SP*-containing gels return to their original shape and the directed motion of the motile gels is arrested. Given this reversible photo-response, the system could exhibit complex dynamic behavior in the presence of non-uniform illumination. To the best of our knowledge, however, there have been no prior theoretical or computational models to uncover this complexity or provide useful guidelines for harnessing the material's unique properties. Herein, we derive a model that captures the salient features of *SP*-containing gels and thus, allows us to predict the spatio-temporal dynamics of these materials. Our model accounts for the kinetics of the photo-induced isomerization of the SP chromophores, and the corresponding decrease in the hydration of the polymer network caused by the isomerization of the chromophores to their spiro form. The approach derived below provides the first theoretical and computational framework for modeling *SP*-containing gels.

We first use our model to study the effects of light on the volume phase transition in *SP*-containing gels and demonstrate good agreement between our findings and corresponding experimental studies,[10] thereby indicating the validity of our approach. We then undertake new studies on the behavior of the SP-modified gels, showing that their reversible, photo-responsive behavior can be harnessed to achieve both dynamically programmable shape-changes and robust, directed motion.

2. Model

In formulating a model for this system, it is important to recall that the spiro form is unstable without the light and hence, in the dark undergoes spontaneous conversion back into the stable, hydrophilic *McH* form:

$$McH \underset{k_D}{\overset{k_L}{\Leftrightarrow}} SP \tag{1}$$

where k_L and k_D are the reaction rates constants for the forward and backward reaction, respectively. Typically, spontaneous conversion back to the *McH* form is significantly slower than the photo-induced isomerization to the spiro form; however, the conversion rates depend strongly on the specific spirobenzopyran derivatives used in the reaction.[12]

The interconversion reaction in Equation (1) is described by the following reaction kinetics:

$$\frac{\partial c_{SP}}{\partial t} = k_L(I(\mathbf{r}))\,(1 - c_{SP}) - k_D c_{SP} \tag{2}$$

where c_{SP} is the concentration of chromophores in the spiro form, *SP*, normalized by the total concentration of chromophores anchored onto the polymer network. The reaction rate constant k_L is proportional to the light intensity at a given point, $I(\mathbf{r})$. Since we focus on thin samples (with a thickness of 60 μm according to the scaling below), we neglect the light attenuation across the thickness of the sample and assume that k_L depends only on the relative location of the illuminated region within the sample. From Equation (2), the photostationary concentration of chromophores in the *SP* form is found as $\tilde{c}_{SP} = (1 + k_D/k_L(I))^{-1}$.

The total energy of the photo-responsive gels consists of the elastic energy of the gel's deformations, U_{el}, and the energy of the polymer-solvent interaction, U_{FH}. We take the energy of the polymer-solvent interaction to be in the following Flory-Huggins form:

$$U_{FH} = \sqrt{I_3}\left[(1-\phi)\ln(1-\phi) + \chi_{FH}(\phi, T)\phi(1-\phi) + \alpha(1-\phi)c_{SP}\right]. \tag{3}$$

The first two terms in Equation (3) describe the mixing energy of the PNIPAAm gel without the chromophores. $\chi_{FH}(\phi, T)$ is the polymer-solvent interaction parameter that depends on the polymer volume fraction, ϕ, and the temperature, T.[16] $I_3 = \det \hat{\mathbf{B}}$ is an invariant of the left Cauchy-Green (Finger) strain tensor $\hat{\mathbf{B}}$ that characterizes the volumetric changes in the deformed gel.[17] The local volume fractions of polymer in the deformed state, ϕ, and undeformed state, ϕ_0, are related as $\phi = \phi_0 I_3^{-1/2}$. We introduce the last term in Equation (3) to describe the photo-induced decrease in the hydration of the polymer network. We assume this term is proportional to the concentration of chromophores in the spiro form, c_{SP}, which we find by solving Equation (2).

The elastic energy contribution, U_{el}, describes the rubber elasticity of the crosslinked polymers,[18,19] and is proportional to the crosslink density, c_0:

$$U_{el} = \frac{c_0 v_0}{2}(I_1 - 3 - \ln I_3^{1/2}), \tag{4}$$

where v_0 is the volume of a monomeric unit and $I_1 = tr\hat{\mathbf{B}}$.[17] Equations (3) and (4) yield the following constitutive equation for the photo-responsive gels:[20]

$$\hat{\sigma} = -P(\phi, c_{SP}, T)\hat{\mathbf{I}} + c_0 v_0 \frac{\phi}{\phi_0}\hat{\mathbf{B}}, \tag{5}$$

where $\hat{\mathbf{I}}$ is the unit tensor, $\hat{\sigma}$ is the dimensionless stress tensor measured in units of $v_0^{-1}kT$, and the isotropic pressure is defined as:

$$\begin{aligned} P(\phi, c_{SP}, T) &= -\left(\phi + \ln(1-\phi) + \chi(\phi, T)\phi^2\right) \\ &\quad + c_0 v_0 \phi (2\phi_0)^{-1} - \alpha c_{SP}\phi. \end{aligned} \tag{6}$$

Here, the parameter $\chi(\phi)$ is related to the Flory-Huggins interaction parameter χ_{FH} in Equation (3) as $\chi(\phi, T) = \chi_{FH}(\phi, T) - (1-\phi)\partial\chi_{FH}(\phi, T)/\partial\phi$. Following ref. [16], we chose $\chi(\phi, T) = \chi_0(T) + \chi_1\phi$, where $\chi_0(T) = [\delta h - T\delta s]/kT$ with δh and δs being the respective changes in the enthalpy and entropy per monomeric unit of the gel.[16]

The dynamics of the polymer network is assumed to be purely relaxational,[20] so that the forces acting on the deformed gel are balanced by the frictional drag due to the motion of the solvent.[21] It is also assumed[20] that the total velocity of the gel/solvent system, $\mathbf{v} \equiv \phi\mathbf{v}^{(p)} + (1-\phi)\mathbf{v}^{(s)} = 0$ and hence, the incompressibility condition, $\nabla\cdot\mathbf{v} = 0$, is automatically satisfied. In other words, the net velocity of the polymer-solvent system is set to zero and it is solely the polymer-solvent inter-diffusion that contributes to the gel dynamics. Thus, the velocity of the polymer network, $\mathbf{v}^{(p)}$, can be found by solving the respective force balance equation and is given by:[20]

$$\mathbf{v}^{(p)} = \Lambda_0(\phi/\phi_0)^{-3/2}(1-\phi)\nabla\cdot\hat{\sigma}. \tag{7}$$

Here, Λ_0 is the dimensionless kinetic coefficient,[20] and the polymer-solvent friction coefficient was chosen as $\xi(\phi) \sim \phi^{3/2}$, which is applicable for a gel in the semi-dilute and intermediate regimes ($\phi < 0.5$).[21] The continuity equation for the polymer volume fraction is

$$\frac{\partial\phi}{\partial t} = -\nabla\cdot(\phi\mathbf{v}^{(p)}), \tag{8}$$

where $\mathbf{v}^{(p)}$ is given by Equation (7).

This photo-responsive gel can attain a steady-state if the following conditions are satisfied: 1) the concentration of the chromophores in the spiro form has reached the photostationary value, $\tilde{c}_{SP}$, and 2) the elastic stresses are balanced by the osmotic pressure, i.e., $\hat{\sigma} = 0$ (see Equation (5). Hence, a steady-state solution for the polymer volume fraction, $\phi_{st}(\tilde{c}_{SP}, T)$, at a given temperature T and a given value of $\tilde{c}_{SP}$, can be found from:

$$\begin{aligned} &c_0 v_0\left[\left(\frac{\phi_{st}}{\phi_0}\right)^{1/3} - \frac{\phi_{st}}{2\phi_0}\right] \\ &= -\left(\phi_{st} + \ln(1-\phi_{st}) + \left[\chi_0(T) + \chi_1\phi_{st}\right]\phi_{st}^2\right) - \alpha\tilde{c}_{SP}\phi_{st} \end{aligned} \tag{9}$$

Here, the left and the right hand sides of Equation (9) represent the elastic stresses for the isotropic three-dimensional deformations and the osmotic pressure, respectively. Hence, we can calculate the equilibrium degree of swelling as a function of $\tilde{c}_{SP}$ at a given temperature as $\lambda_{eq}(\tilde{c}_{SP}, T) = (\phi_0/\phi_{st}(\tilde{c}_{SP}, T))^{1/3}$.

The above evolution equations are discretized and solved numerically by adapting our three-dimensional gel Lattice Spring Model (gLSM)[22] to this photo-reactive system. Within the framework of this gLSM, a gel sample is represented by a set of general lineal hexahedral elements.[23,24] Initially, the sample is undeformed and consists of $(L_x-1)\times(L_y-1)\times(L_z-1)$ identical cubic elements; here, L_i is the number of nodes in the i-direction, $i = x, y, z$. In the undeformed state, each element is characterized by the same volume fraction ϕ_0 and crosslink density c_0. Upon deformation, the elements move together with the polymer network so that the amount of polymer and number of crosslinks within each hexahedral element remain equal to their initial values. The details of the three-dimensional gLSM, as well as validation of the approach, can be found in ref. [22]. Originally the gLSM approach[20,25] was developed to describe the elastodynamics and reaction-diffusion processes occurring within gels undergoing the Belousov-Zhabotinsky (BZ) reaction, the so-called "BZ gels".[26,27] Using this model, we obtained qualitative agreement between the findings from our calculations[22,28–30] and various experimental observations on BZ gels.[22,28–31] Most recently, we developed a hybrid model based on the gLSM approach to simulate the behavior of microscopic posts that were embedded in a thermo-responsive gel and interacted with a phase-separated solvent. The simulation results obtained with this approach are in a good agreement with the corresponding experimental data.[32] Via the above equations, we herein extend our three dimensional gLSM[22] to account for the effect of visual light on *SP*-containing gels.

To describe the gel properties, we chose the volume fraction of the undeformed gel to be $\phi_0 = 0.08$ and the dimensionless crosslink density was taken to be $c_0 v_0 = 1.35\times10^{-3}$; these values correspond to the experimental values provided in ref. [10] for *SP*-functionalized PNIPAAm gels. Specifically, these values correspond to 84.0 mg of NIPAAm monomer and 5.8 mg of *N,N′*-methylene(bis)acrylamide (BAAm) crosslinker dissolved in 1 mL of solvent, as detailed in the Supporting Information of ref. [10]. (The *SP*-functionalized gels were synthesized by free-radical polymerization with ammonium peroxodisulfate (APS) as an initiator and *N,N,N′,N′*-tetramethylethylenediamine (TEMED) as the catalyst; for further details of the synthesis, we refer the reader to the experiments in ref. [10]).

For the gel-solvent interaction parameters, we set $\chi_1 = 0.518$ and calculated $\chi_0(T)$ as specified above using the values for the changes in the enthalpy and entropy per monomeric unit of the network given in ref. [16] (based on experimental swelling data for neutral PNIPAAm gels) as $\delta h = -12.4\times10^{-14}$ and $\delta s = -4.7\times10^{-16}$. With these values, the equilibrium degree of swelling in the dark at $T = 20\,^{\circ}\mathrm{C}$ can be calculated as $\lambda_{eq}(0, 20) = 1.054$. Finally, we set the interaction parameter that describes the photo-induced decrease in the hydration of the polymer network to $\alpha = 8.25\times10^{-2}$. The latter parameter is the only fitting parameter in the model; its value was chosen to produce a light-induced decrease in the gel's degree of swelling that is similar in magnitude to the corresponding experimental values.[10]

For the reference values of the forward and backward reaction rate constants, we used $k_L = 0.5$ and $k_D = 0.05$, respectively; at these values, the photo-stationary concentration of chromophores in the spiro form is $\tilde{c}_{SP} \approx 0.91$. This value is within the range provided in ref. [12], where researchers demonstrated that the isomerization from the *McH* to the *SP* form in the photo-stationary state ranged from 82% to 98%, depending on the specific spirobenzopyran derivatives that were used. The incomplete ring closure (i.e., incomplete conversion to *SP* form) was attributed to the concurrent spontaneous ring opening taking place under the irradiation. In the same study,[12] the researchers reported a range of the reaction rate constants for the spontaneous ring opening in the dark from $\sim 10^{-2} s^{-1}$ to $5 \times 10^{-4} s^{-1}$ for different spirobenzopyran derivatives. Here, we relate our reference value of $k_D = 0.05$ to the experimental value of $\sim 10^{-2} s^{-1}$ and hence, we set our dimensionless unit of time to be $T_0 \approx 5s$. Finally, we take the dimensionless unit of length to be $L_0 = 30\mu m$.

To compare the characteristic re-swelling time of our simulation sample to the experimental study,[12] we set $T = 25\,^{\circ}C$ and first illuminate a simulation sample of size $10 \times 10 \times 10$ nodes (cube height of $\approx 0.3mm$) using all the reference values provided above. After the system has reached equilibrium, we turn off the illumination and calculate the characteristic relaxation time, τ^*_{sw}, by fitting the dynamics of the average degree of swelling with a single exponent. We obtain $\tau^*_{sw} \approx 24$, which corresponds to $\approx 120s$ in physical units; this value is in the reasonably good agreement with the experimental value of $\approx 133s$ provided in ref. [12] for cylindrical gels with a diameter of $0.3\,mm$[33] and with the reaction rate constant of $\sim 10^{-2} s^{-1}$ at the same temperature of $T = 25\,^{\circ}C$. It is worth noting that by using significantly lower values of k_D in our studies than our reference value, we can also readily reproduce the much slower re-swelling kinetics that was observed for the remaining gel samples in ref. [12]. Finally, the reference size of our simulation sample was chosen as $50 \times 50 \times 3$ nodes (using the notation in ref. [22], which corresponds to a size of $1.47mm \times 1.47mm \times 0.06mm$ in the dark at $\delta\lambda = \left(\lambda_{eq}(0, T) - \lambda_{eq}(\tilde{c}_{SP}, T)\right) / \lambda(0, T)$.

We emphasize that the physical origin of the photo-induced volume changes of the gels we focus on here is distinctly different from that in cases where the collapse of the gel with different chromophores resulted from a direct light-induced heating.[36,37] Here, the temperature in the sample remains constant during the illumination[10] and the light-induced change in the conformation of the chromophores results directly in a decrease in the hydration of the gels;[10] it is this effect that we exploit in creating programmable reconfiguration and motion of gels.

3. Results and Discussion

We first focus on the effect of light on the volume phase transition in *SP*-containing gels and compare our findings with the corresponding experimental data. **Figure 1**a shows the equilibrium degree of swelling, $\lambda_{eq}(\tilde{c}_{SP}, T)$, normalized by its value in the dark at $T = 20$ °C. Specifically, in Figure 1a, we plot $\tilde{\lambda}_{eq} \equiv \lambda_{eq} / \lambda_{eq}(0, 20)$ in the absense of light (black line) and for two values of $\tilde{c}_{SP}$ (red and blue lines).

Notably, our simulations are in good agreement with the relevant experimental findings.[10] Namely, **Figure 2**a in ref. [10] shows experimental data on the equilibrium size of *SP*-functionalized gels as a function of temperature in the dark and under illumination with light of a fixed intensity of $I = 5$ mW/cm^2 and clearly demonstrates both the decrease in the degree of swelling and a significantly smoother volume phase transition in the presence of the light. Our simulations also show that the latter effects are more pronounced for higher ratios between the forward and backward reaction rate constants (and hence higher values of $\tilde{c}_{SP}$), as can be seen by comparing the red and blue curves, for which $k_L(I)/k_D = 1$ and $k_L(I)/k_D = 10$, respectively.

The solid lines in Figure 1a represent exact analytical solutions, where we first obtain ϕ_{st} from Equation (9), and then calculate $\lambda_{eq} = (\phi_0/\phi_{st})^{1/3}$. The symbols in Figure 1a represent the simulation data. The excellent agreement between our analytical solution and simulation data indicate the accuracy of our simulation approach. Using a sample of size $3 \times 3 \times 3$ nodes, the data points in Figure 1a were obtained by a stepwise increase in temperature, with a small increment of $\Delta T = 0.02$ (from its initial value of $T = 20\,^{\circ}C$) during each time interval of 200 dimensionless time units. Here, we plot the degree of swelling at the end of these time intervals, λ_{eq}, normalized by its value at 20 °C. The results are independent of the value of ΔT and on the length of this time interval, as long as it is sufficiently large that the gel reaches equilibrium for the given value of T.

As can be seen from the inset in Figure 1a, the relative light-induced decrease in the degree of swelling, $\delta\lambda = \left(\lambda_{eq}(0, T) - \lambda_{eq}(\tilde{c}_{SP}, T)\right) / \lambda_{eq}(0, 20)$, increases with increases in T until it reaches a peak value at a phase transition temperature. Further increases in T lead to a sharp decrease in $\delta\lambda$. This distinctive behavior of $\delta\lambda$ is in a good agreement with the corresponding experimental findings.[10] In particular, we compare our simulation results to the experimental data provided in Figure 2b of ref. [10] on the relative change in equilibrium size as a function of temperature at a fixed light intensity of $I = 5$ mW/cm^2. The experiments clearly show:[10] 1) a smooth increase in the relative change in the equilibrium size with an increase in temperature at low temperatures, until this value reaches a pick at the phase transition temperature, and 2) a sharp decrease in the relative change in equilibrium size with further increases in temperature, until this value reaches zero at approximately $T = 35$ °C. Our simulation results in the inset in Figure 1a are in good agreement with the above observations. Finally, we note the correspondence between the experimental[10] and simulation values for the absolute value of the relative change in equilibrium size. In the experimental studies, at $T = 21$ °C, the size of the sample decreased by 24% (at fixed light intensity). For the reference case in our simulations, this value is about 20% at the same temperature (see Figure 1a, blue curve).

To the best of our knowledge, these simulations constitute the first theoretical or computational determination of the volume phase transition in *SP*-containing gels. Good agreement between our results and available experimental data[10] indicates the validity of our approach, which we then use to undertake the studies described below.

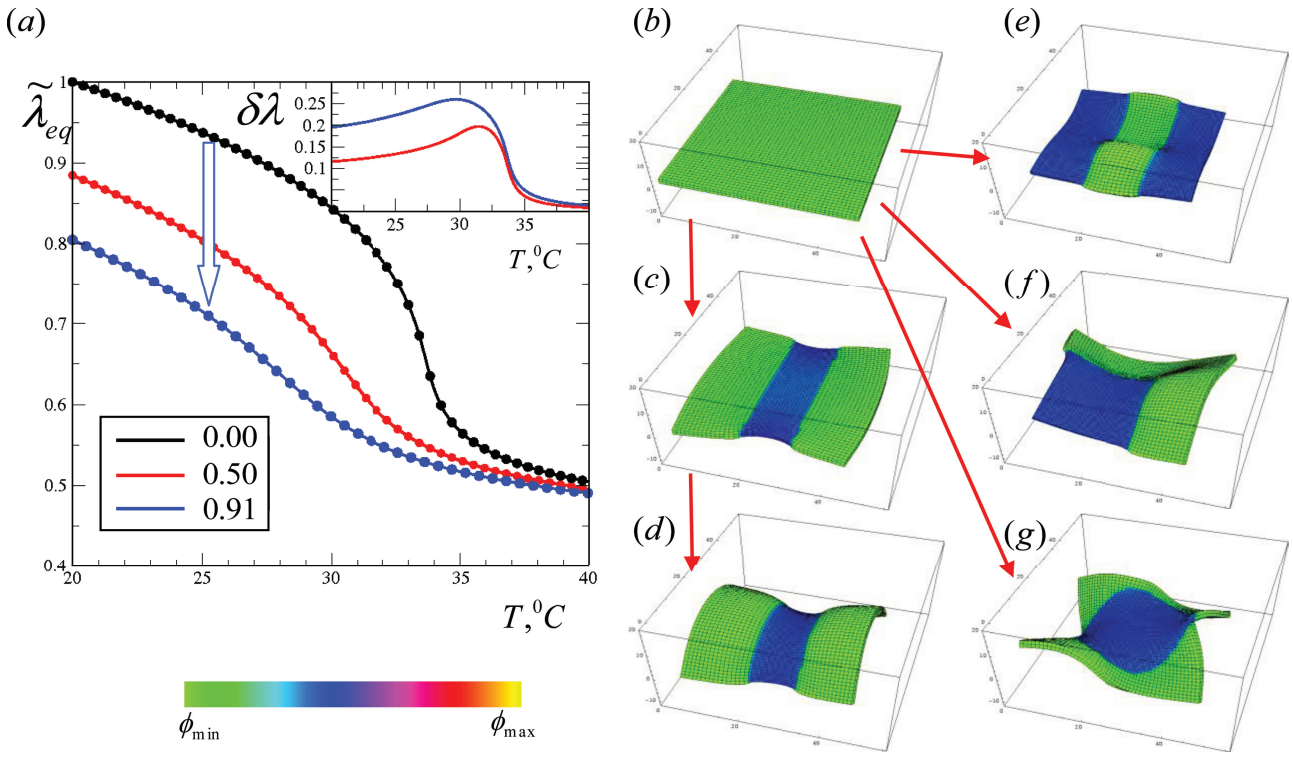

Figure 1. (a) Volume phase transition in gels in the dark (black curve) and upon illumination (red and blue curves), with the values $\tilde{c}_{SP}$ given in the legend. Inset shows relative light-induced shrinking, $\delta\lambda = (\lambda_{eq}(0,T) - \lambda_{eq}(\tilde{c}_{SP},T))/\lambda(0,T)$. (b) Sample in the dark (c–g) Sample under non-uniform illumination; illuminated regions are shrunk and are shown in dark blue. In the color bar, $\phi_{min} = 0.08$ and $\phi_{max} = 0.35$. The size of the sample is $50 \times 50 \times 3$ nodes, which corresponds to $1.47mm \times 1.47mm \times 0.06mm$ at T = 25 °C . The dimensionless times for which the sample is illuminated are $t = 4 \times 10^3$ in (c) and $t = 5.6 \times 10^5$ in (d–g). One dimensionless unit of time corresponds to $T_0 \approx 5s$ and one dimensionless unit of length corresponds to $L_0 = 30\,\mu m$; details of the scaling relationships between the dimensionless units and experimental values are given in the Model section.

The photo-induced shrinking provides a means to not only "mold" the gels into a particular shape, but also dynamically reconfigure this material. For example, a certain shape can be achieved by illuminating the gels through a photomask with a specific opening. This shape can then be dynamically altered by shifting to a photomask with a different opening, as illustrated in Figure 1b–g. Here, we set $T = 25\,^{\circ}C$ and $k_L(I)/k_D = 10$ within the illuminated regions. The sample remains flat in the absence of illumination (Figure 1b), but can be "molded" into variety of shapes (Figure 1c–g) as we change the openings in the mask and illuminate the sample.

There are a number of processes occurring on different time scales upon illumination of the sample. The fastest process is the conversion of chromophores into the spiro form within the illuminated regions. This process results in the increase of c_{SP} until it plateaus at its photo-stationary value, $\tilde{c}_{SP}$; the characteristic time scale for this process is $(k_L + k_D)^{-1}$ (see SI, Figure S1). This photo-conversion results in the shrinking of the sample within the illuminated region until the polymer volume fraction within this region approaches its respective equilibrium value, φ_{eq}; this process depends on the gel's mobility and size, and is slower than the photo-conversion (see SI, Figure S1). The structural changes that result from these processes can be seen in Figure 1c, which shows the early time morphology of a sample after illumination through a rectangular opening. At this relatively early stage, the sample consists of regions with different degrees of swelling, but the entire sample lies essentially in one plane. Further evolution of the sample leads to out-of-plane distortions, so that at late times, the sample reaches the steady-state morphology shown in Figure 1d. (Intermediate steps of the morphology development for this case are shown in the SI, Figure S1)

Figures 1e–g clearly show that the uniform sample in Figure 1b can be reconfigured into variety of shapes by altering the openings in the photomask. Additional examples of shapes that can be formed from the same sample in Figure 1b are provided in the SI (see Figure S2). These shapes can be further altered by changing the light intensity or temperature. (Varying the latter parameters alters the ratio between the equilibrium degree of swelling in the dark and in the light, and consequently defines the late time morphology.) Notably, the shapes shown in Figure 1c–g resemble shapes observed in gels that encompass gradients in crosslink density or variations in the local fraction of polymer at the time of preparation.[3–6] Here, however, well-defined regions with different degrees of swelling are introduced dynamically by non-uniform illumination onto the initially uniform, homogeneous gel sample, and hence, multiple shapes can be written and rewritten into the same sample due to the complete reversibility of the process.

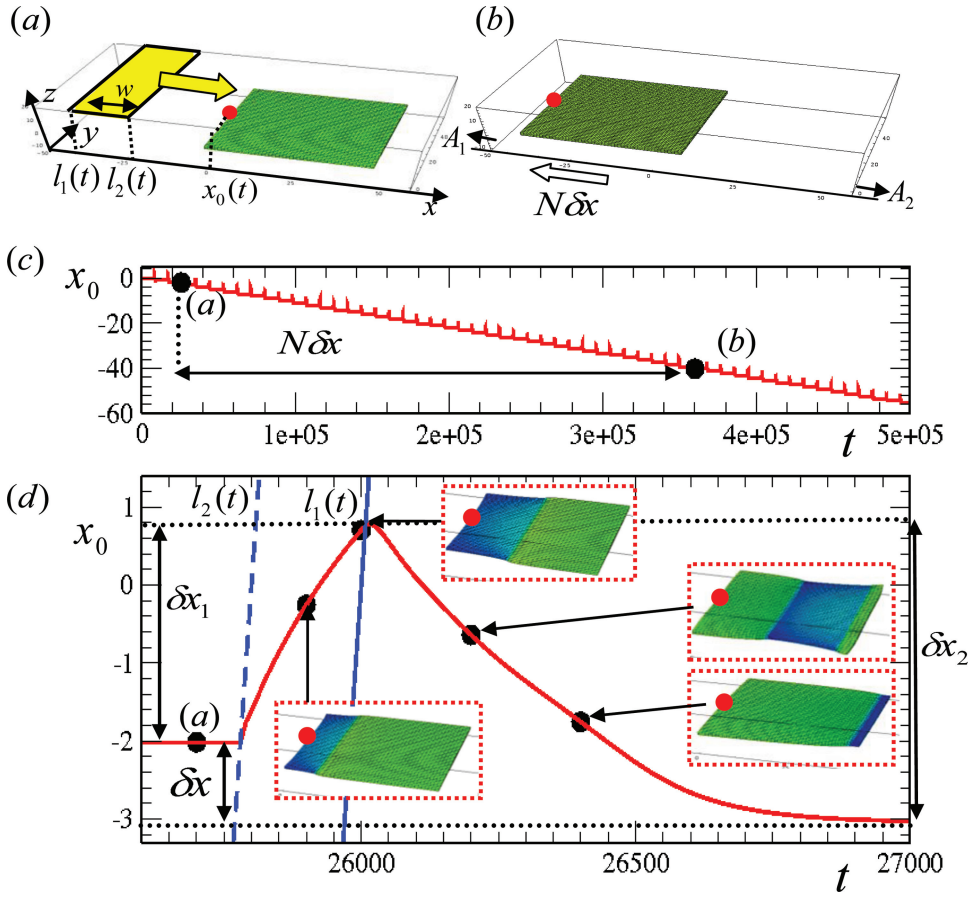

Figure 2. (a,b) Sample positions before (a) and after (b) N pass of the light from left to right (from $A_1 = -800$ till $A_2 = 100$). (c,d) The x-coordinate of the central node on the front face of the gel, $x_0(t)$ (the node is marked by red circle in (a,b). The values of $x_0(t)$ corresponding to the images in (a,b) are marked by dark circles in (c). Times corresponding to insets in (d) are as following: $t = 2.59 \times 10^5$, $t = 2.60 \times 10^5$, $t = 2.62 \times 10^5$, and $t = 2.64 \times 10^5$.

Since the light induced "patterning" and shape changes are achieved by altering the gel's hydrophilicity and do not lead to any notable changes in temperature,[10,11] we can inscribe distinct features that are on the micron to submillimeter length scales. This level of patterning would not be feasible in photoresponsive gels where light causes the deswelling through a local heating.[36,37] This is because thermal diffusion is much faster than the collective diffusion of the polymer network.[36,38] (Taking the characteristic thermal diffusivity in the hydrogels[38] to be approximately $2.3 \times 10^{-7} m^2/s$, we can estimate that the temperature equilibrates during $\approx 0.4s$ within a characteristic length of $\approx 300\,\mu m$, prohibiting formation of sharp patterns by light-induced heating and causing more uniform heating and shrinking of the entire sample.)

The anchored chromophores introduce another remarkable feature of this system: in the presence of spatially and temporally varying light, the photosensitive gel can undergo autonomous, directed motion, as illustrated in Figure 2. Starting with an initially non-illuminated sample, we repeatedly move a light source from the left to the right, as marked by the yellow arrow in Figure 2a. Specifically, the sample is illuminated through a relatively narrow rectangular opening in a photomask (with a width of $w = 20$) and this opening is rastered over the sample so that its left edge, $l_1(t)$, is moved from A_1 to A_2 along the x-direction with a speed v_L. Similar to the examples above, when the opening is located directly over a specific area, the light causes that region to shrink. With a shift of the light to the right, the region that is now in the dark swells, and the newly illuminated region shrinks. The continual swelling/shrinking of contiguous regions results in the directed movement of the sample. As can be seen in Figure 2b, after multiple passes (i.e., a total of N passes) of the stripe of light, the gel undergoes a net displacement to the left (as marked by the open arrow).

To help visualize the sample's motion, the central node on the front face of the gel is marked by a red dot. The x-coordinate of this point, $x_0(t)$, is plotted as a function of time in Figure 2c and clearly shows multiple small-scale oscillations. A blow up of $x_0(t)$ for a single period reveals that the gel's net motion to the left consists of a movement to the right (δx_1 in Figure 2d) and a higher amplitude motion to the left (marked as δx_2). The blue lines in Figure 2d ($l_1(t)$ and $l_2(t)$) mark the positions of the edges of the light stripe as a function of time as this stripe moves over the sample. Note that the value of $l_1(t)$ varies during a single swipe from $A_1 = -800$ until $A_2 = 100$

dimensionless units here and in the simulations below unless specified otherwise. (In Figure 2d we show only the fraction of the $l_1(t)$ and $l_2(t)$ that correspond to the time when the stripe is located close to front edge of the sample.)

When the right edge of the stripe of light approaches the gel's front face, it causes a shrinking of that portion and the sample is shifted towards the right (in the positive x-direction). As long as our reference point (red circle in Figure 2) remains illuminated, its coordinate, $x_0(t)$, increases with time and the sample moves in the same the direction as the light. When the light moves beyond this point, however, the frontal portion begins to re-swell back to its equilibrium value and the sample moves to the left (in the negative x-direction), as seen in Figure 2d.

Figure 2d indicates that $x_0(t)$ reaches its maximum value within a single swipe when the light moves over this reference point (the red dot); namely, the when the position of the back edge of the stripe, $l_1(t)$, is equal to $x_0(t)$. Figure 2d also shows that the displacement of this point during the gel's shrinking and swelling occurs asymmetrically ($\delta x_1 < \delta x_2$). Recall that the gel moves due to the inter-diffusion of the solvent and polymer;[20,39,40] hence, the motion of solvent in one direction causes movement of the polymer in the opposite direction. When the sample undergoes re-swelling due to the stripe motion to the right (see the two insets on the right in Figure 2d), the solvent intake by the previously shrunken portion is unrestricted at the left edge and restricted on the right edge of the sample. As the light is moved from left to right, the solvent is effectively "pushed" to the right; this net movement of solvent causes the polymer to move in the opposite direction, i.e., the polymer moves to the left. (In previous studies, we showed that the propagation of a traveling chemical wave in one direction resulted in the overall movement of the polymer in the opposite direction;[40–43] this motion was also caused by the polymer-solvent inter-diffusion.[40–43] Notably, the gel moves only when a portion of the sample is illuminated or directly after the light was shifted and the gel swells until it reaches its equilibrium size. Since we move the light source over a relatively wide distance ($l_1 \in [A_1 : A_2]$ as marked schematically in Figure 2), the plot of $x_0(t)$ shows distinct regions where the sample remains stationary between the motions during each swipe (see Figure 2c,d).

This light-induced motion is robust and is observed for a wide range of parameters. To characterize the gel's motion quantitatively, we calculate the net displacement, δx (see Figure 2d) during a single swipe, and the average velocity of the sample's motion during that swipe, $v_g = \delta x)\,\delta\tau$, where $\delta\tau$ is the time interval between the beginning and end of the gel's motion. We calculate the time interval $\delta\tau$ from our simulation data as the interval between the moments in time when the gel displacement satisfies $|x_0(t+1) - x_0(t)| > 5 \cdot 10^{-4}$ (i.e., we cut off the time intervals when the gel remains stationary). We first vary the rastering velocity, v_L, and calculate δx and v_g for a range of values of v_L. **Figure 3**a shows that there is a range of rastering velocities, v_L, yielding a relatively rapid displacement of the gel (and resulting in the peak values on the red curve, v_g). At slow rastering velocities, the displacement of the sample, δx, increases since the gel has a significantly longer time to swell and deswell in response to the change in illumination; however, the entire process takes a longer time, resulting in a decrease of v_g. (This can be seen from Figure S3a in the SI that shows the displacement of the front edge of the sample during a single swipe of the light with a velocity $v_L = 0.005$, which is significantly smaller than our reference

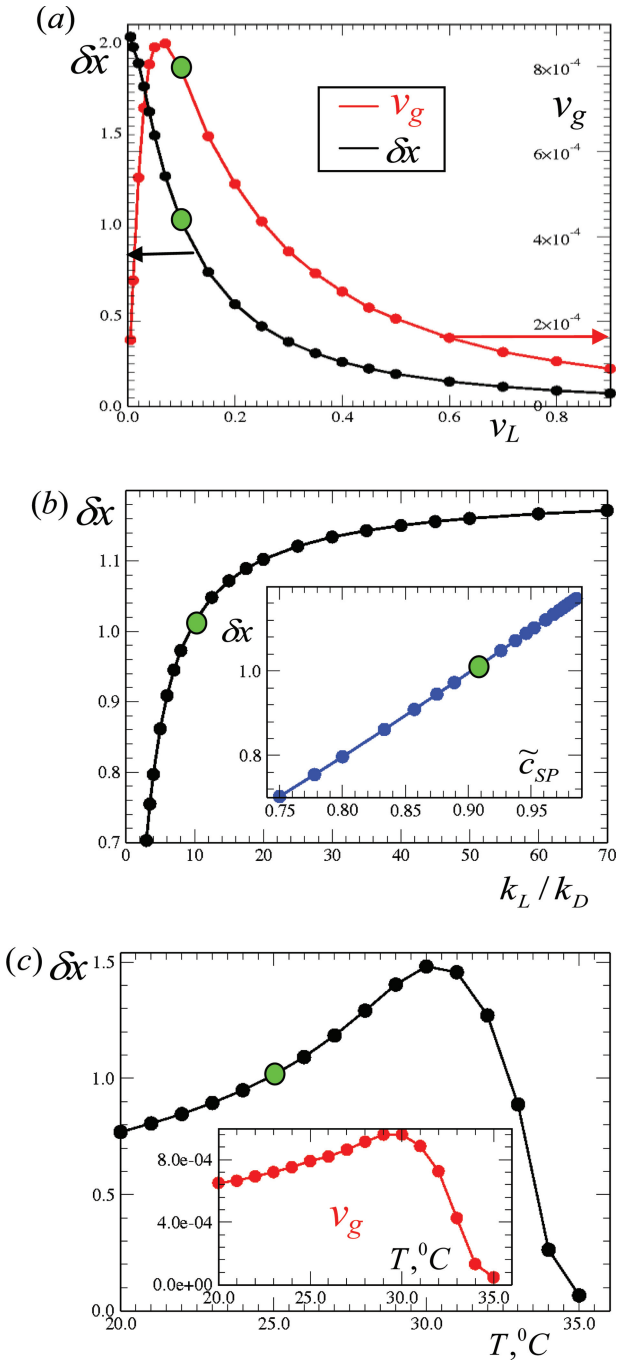

Figure 3. Displacement of the sample during a single swipe, δx, as a function of v_L in (a), of k_L/k_D in (b), and of T in (c). The red curve in (a) corresponds to gel velocity, $v_g(v_L)$, with values marked on the right axes. The insets in (c) and (d) give $\delta x(\tilde{c}_{SP})$ and $v_g(T)$, respectively. The data points corresponding to the case in Figure 2 are marked in (a–c) by green circles.

value, $v_L = 0.1$. Here, both δx_1 and δx_2 are larger than the values in the reference case in Figure 2d, but the swipe takes a significantly longer time so that effective v_g is lower.) Conversely, at higher v_L, the gel never reaches its equilibrium polymer volume fraction at a given light intensity because the illumination is moved over the sample much faster then the characteristic response time of the gel (see Figure S3b,c in SI). Hence at high v_L, we still observe the motion to the left but both δx and v_g decrease significantly with respect to the optimal values observed at intermediate velocities.

We now fix the velocity of motion of the stripe at $v_L = 0.1$ and vary the ratio k_L/k_D (see Figure 3b); increases in the value of k_L can be achieved by increasing the light intensity. The displacement during a single swipe, δx, increases with the increase in k_L/k_D until it reaches a plateau. Similarly, v_g also increases and reaches a plateau (not shown). This plateau corresponds to the values of k_L/k_D at which all the available chromophores are converted into the spiro form (i.e., $\tilde{c}_{SP} \sim 1$). The displacement δx scales approximately linearly with the value of $\tilde{c}_{SP}$ as can be seen in the inset to Figure 3b.

Finally, we fix both $k_L/k_D = 10$ and $v_L = 0.1$, and vary the temperature of the sample (see Figure 3c). We find that δx increases with T until it reaches the phase transition temperature; further heating, however, leads to a decrease in δx. The bell-shaped plots of $\delta x(T)$ and $v_g(T)$ (see inset in Figure 3c) closely resemble the plot of $\delta\lambda(T)$ (inset in Figure 1a). This is because the gel's motion results from the light-controlled shrinking and swelling of the sample, and hence the velocity of this motion is highest for the value of T at which the difference between the equilibrium size of the gel with and without light is the highest.

The above results show that the gel's motion can be effectively controlled by altering the velocity of the light source, light intensity (i.e., k_L) or temperature of the sample. The observed dependence of δx on temperature implies that if a sample is placed in a temperature gradient, then rastering with light over portions of the sample experiencing different temperatures will result in their motion with effectively different speeds. To illustrate the consequences of this behavior, we now place a ring-shaped sample in a temperature gradient, with the highest temperature, T = 30 °C being on the top of the box shown in **Figure 4**a (at z = 40) and with the lowest temperature, T = 20 °C, being on the bottom of this box (at z = 20). The sample size is $180 \times 8 \times 3$ and the initial swelling of this sample corresponds to T = 25 °C. This sample has a relatively small region with a higher crosslink density (the bottom portion of this region is indicated by the red circle in Figure 4a); by following the displacement of this region, one can more clearly visualize the shape changes and displacement of the sample.

Similar to the behavior shown in Figure 2, repeated motion of the light source over the sample from the left to the right (indicated by the yellow arrow) induces the net motion of the sample to the left (Figure 4a). The imposed temperature gradient, however, significantly alters the shape and motion of this gel. In particular, the temperature gradient gives rise to a greater shrinking of the portion of the sample that is at the higher temperature (as can be understood from Figure 1a). The additional, dramatic effects of the temperature gradient can be explained as follows. If the ring in Figure 4a were held

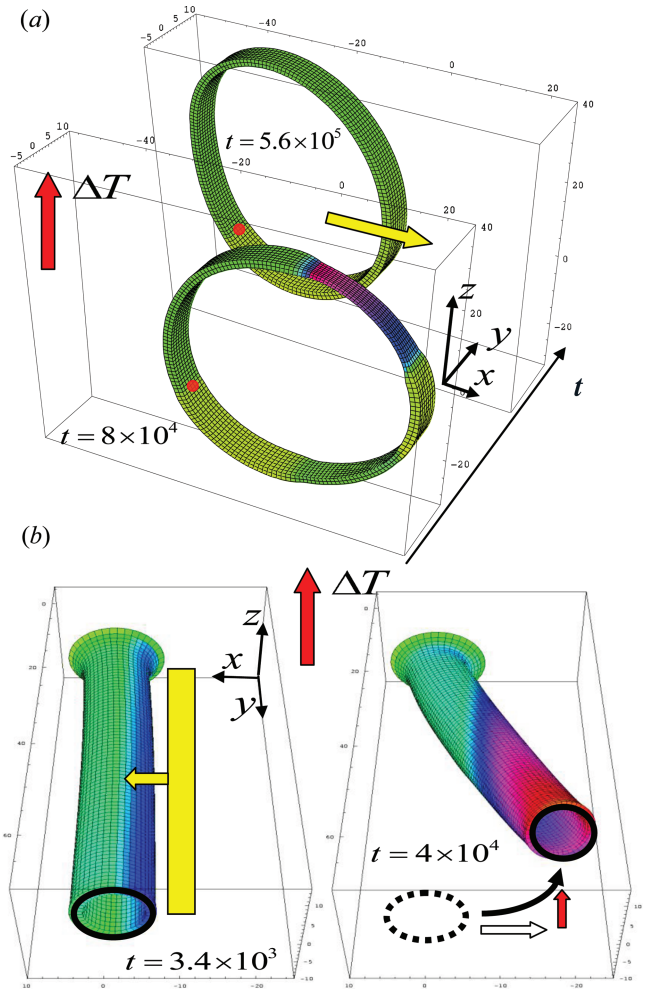

Figure 4. (a,b) Repeated motion of illuminated region over the sample placed in a temperature gradient results in the superposition of the motion in the direction opposite to the motion of light and motion towards higher temperature (upwards). Here, we use the same color bar as given in Figure 1, but set ϕ_{max} = 0.23. For the ring structure, the collapsed region at early times indicates the influence of the light. The image at late times is taken at a point where the light is away from the gel.

at a constant, uniform temperature, it would move uniformly to the left along the x-direction (due to the light), without any displacement in the vertical direction. The velocity of this motion, however, depends on temperature, as given in the inset in Figure 3c. Within the range of temperatures considered in Figure 4a, the velocity of the sample increases with the increase in T. Hence, when the sample is placed in a temperature gradient, the top portion of the sample moves to the left with a slightly higher velocity (according to Figure 3c) and thus, gives rise to a distorted shape where the upper portion of the ring effectively "leads" the movement. Hence, in subsequent swipes, the light now moves over a distorted, slightly elongated sample (rather than the initial ring-shaped object). The top of the elongated sample extends higher along the temperature gradient and again moves with a higher velocity, so that this top portion too appears to lead the movement. Further swipes of the light of

over the sample continue to amplify this effect until ultimately, more and more of the sample is driven towards the higher temperatures. Consequently, at late times, the sample exhibits a net displacement not only to the left, but also upwards. This net motion can clearly be seen by comparing the front and back images in Figure 4a for the respective early and late time positions of the gel.

The distinctive features of the gel's light-induced motion within a temperature gradient are robust and are observed for a wide variety of sample shapes. Furthermore, the motion occurs in a similar manner even when one end of the sample is anchored to a wall. Additionally, the direction of the sample's motion can be controlled by specifying the directionality of the rastering light. To illustrate these points, in our final example, we consider a tubular sample that is anchored to a wall by one end; the temperature gradient within the system is indicated by the arrow in Figure 4b. Instead of moving the light from left to right as in the examples above, we now move the light source over the entire sample from right to left (as shown by the yellow stripe in Figure 4b). The sample size is $40 \times 80 \times 3$ nodes, the initial swelling of this sample corresponds to $T = 25$ °C, and we set the rastering range as $A_1 = -40$ and $A_2 = 9$. We now observe the bending of the free end to the right due to the rastering light and to the top because of the temperature gradient. The displacement of the free end is marked schematically in the right image in Figure 4b where the dashed line indicates the initial position and the black arrow marks the observed displacement, which consists of contributions to the net motion caused by the motion of the light source (marked by the open white arrow) and by the presence of the temperature gradient (marked by the red arrow). (See Figure S4 for the trajectory of the sample's free end with and without the temperature gradient.) Figure 4b also shows that the portion of the gel at the higher temperature is more collapsed than the rest of the gel, as would be anticipated from Figure 1a.

Figure 4b illustrates that by using combinations of non-uniform illumination and temperature, one can effectively control the position of the free end of this tubular gel. Hence, this procedure could be used to remotely and non-invasively connect or re-connect spatially isolated materials. This feature can be advantageous in the systems that require soft flexible connections between, for example, multiple reaction chambers with different reagents. In effect, remote docking of the tube-shaped samples could ultimately allow one to regulate the transport of species though complex, flexible assemblies.

3. Conclusions

Our simulations show that the motion of a light source over gels containing spirobenzopyran chromophores induces a well-defined expansion and contraction along the sample and results in its directed motion. By repeatedly moving this light in a specific direction along the gel, we could drive samples of different shapes to undergo a net displacement in a well-defined manner. The ability to remotely manipulate both the shape of the sample and its directed motion is critical for driving multiple samples to "recognize" each other and to ultimately "dock" to form soft, self-assembled structures with distinctive architectures. We emphasize that the shape-changes and guided motion of *SP*-functionalized polymer gels driven by the non-uniform illumination described in this work have not yet been observed experimentally and are predictions of our simulation studies. Importantly, this predicted light-controlled shape-changing and guided motion opens new routes for fabricating a range of dynamically reconfigurable materials. In particular, this "molding" technique permits the assembled pieces to be re-shaped and hence, the same sample can be used or reused for a range of different functionalities. In effect, the technique ascribes the material with a remarkable adaptability: the ability to change shape (and function) with a change in environment.

Supporting Information

Supporting Information is available from the Wiley Online Library or from the author.

Acknowledgements

ACB gratefully acknowledges financial support from the DOE.

Received: December 30, 2012
Revised: June 25, 2013
Published online: July 31, 2013

[1] M. D. Norman, J. Finn, T. Tregenza, *Proc. Roy. Soc. B. Biol. Sci.* **2001**, *268*, 1755.
[2] J. J. Allen, L. M. Mathger, A. Barbosa, R. T. Hanlon, *J. Comp. Physiol. A.* **2009**, *195*, 547.
[3] J. Kim, J. A. Hanna, R. C. Hayward, C. D. Santangelo, *Soft Matter* **2012**, *8*, 2375.
[4] D. P. Holmes, M. Roche, T. Sinha, H. A. Stone, *Soft Matter* **2011**, *7*, 5188.
[5] Y. Klein, E. Efrati, E. Sharon, *Science* **2007**, *315*, 1116.
[6] J. Kim, J. A. Hanna, M. Byun, C. D. Santangelo, R. C. Hayward, *Science* **2012**, *335*, 1201.
[7] W. M. Huang, Z. Ding, C. C. Wang, J. Wei, Y. Zhao, H. Purnawali, *Mater. Today* **2010**, *13*, 54.
[8] I. Bellin, S. Kelch, R. Langer, A. Lendlein, *Proc. Natl. Acad. Sci. USA* **2006**, *103*, 18043.
[9] T. Xie, *Nature* **2010**, *464*, 267.
[10] A. Szilagyi, K. Sumaru, S. Sugiura, T. Takagi, T. Shinbo, M. Zrinyi, T. Kanamori, *Chem. Mater.* **2007**, *19*, 2730.
[11] T. Satoh, K. Sumaru, T. Takagi, T. Kanamori, *Soft Matter* **2011**, *7*, 8030.
[12] T. Satoh, K. Sumaru, T. Takagi, K. Takai, T. Kanamori, *Phys. Chem. Chem. Phys.* **2011**, *13*, 7322.
[13] L. Florea, D. Diamond, F. Benito-Lopez, *Macromol. Mater. Engin.* **2012**, *297*, 1148.
[14] In non-acidic environments, the spiropyran derivatives are typically in the closed-ring (spiro, or SP) form and undergo UV-light initiated conversion to the open-ring (merocyanine, or MC) form (i.e., conversion). The merocyanine form, however, is unstable without UV irradiation; hence, without illumination with the UV light, a conversion back to the spiro form, is observed.
[15] S. Sugiura, K. Sumaru, K. Ohi, K. Hiroki, T. Takagi, T. Kanamori, *Sens. Actuat. A: Phys.* **2007**, *140*, 176.

[16] S. Hirotsu, *J. Chem. Phys.* **1991**, *94*, 3949.
[17] R. J. Atkin, N. Fox, *An Introduction to the Theory of Elasticity*, Longman, New York **1980**.
[18] T. L. Hill, *An Introduction to Statistical Thermodynamics*, Addison-Weley, Reading, MA **1960**.
[19] A. Onuki, *Adv. Polym. Sci.* **1993**, *109*, 63.
[20] V. V. Yashin, A. C. Balazs, *J. Chem. Phys.* **2007**, *126*, 124707.
[21] B. Barriere, L. Leibler, *J. Polym. Science Part B: Polymer Physics* **2003**, *41*, 166.
[22] O. Kuksenok, V. V. Yashin, A. C. Balazs, *Phys. Rev. E* **2008**, *78*, 041406.
[23] I. M. Smith, D. V. Griffiths, *Programming the Finite Element Method*, Wiley, Chichester, England **2004**.
[24] O. C. Zienkiewicz, R. L. Taylor, *The Finite Element Method*, Vol. *1*, Butterworth-Heinemann, Oxford, England **2000**.
[25] V. V. Yashin, A. C. Balazs, *Science* **2006**, *314*, 798.
[26] R. Yoshida, T. Takahashi, T. Yamaguchi, H. Ichijo, *J. Am. Chem. Soc.* **1996**, *118*, 5134.
[27] R. Yoshida, S. Onodera, T. Yamaguchi, E. Kokufuta, *J. Phys. Chem. A.* **1999**, *103*, 8573.
[28] I. C. Chen, O. Kuksenok, V. V. Yashin, R. M. Moslin, A. C. Balazs, K. J. Van Vliet, *Soft Matter* **2011**, *7*, 3141.
[29] P. Yuan, O. Kuksenok, D. E. Gross, A. C. Balazs, J. S. Moore, R. G. Nuzzo, *Soft Matter* **2013**, *9*, 1231.
[30] O. Kuksenok, V. V. Yashin, M. Kinoshita, T. Sakai, R. Yoshida, A. C. Balazs, *J. Mater. Chem.* **2011**, *21*, 8360.
[31] R. Yoshida, M. Tanaka, S. Onodera, T. Yamaguchi, E. Kokufuta, *J. Phys. Chem. A.* **2000**, *104*, 7549.
[32] X. M. He, M. Aizenberg, O. Kuksenok, L. D. Zarzar, A. Shastri, A. C. Balazs, J. Aizenberg, *Nature* **2012**, *487*, 214.
[33] We note that the characteristic swelling time is expected to be higher for a cylindrical gel than for a spherical gel of the same diameter; this ratio between the swelling times depends on the aspect ratio of the cylindrical gel and for example is roughly 1.8 for infinitely long cylinders.[34,35] In these estimates, we simply require that the characteristic swelling times of the cubic sample in the simulations be of the same order as that of the cylindrical sample with the same diameter in the experiments.
[34] Y. Li, T. Tanaka, *J. Chem. Phys.* **1990**, *92*, 1365.
[35] K. Urayama, N. Murata, S. Nosaka, M. Kojima, T. Takigawa, *Prog. Colloid. Polym. Sci.* **2009**, *136*, 107.
[36] A. Suzuki, T. Tanaka, *Nature* **1990**, *346*, 345.
[37] A. Suzuki, *Adv. Polym. Sci.* **1993**, *110*, 199.
[38] M. Guenther, G. Gerlach, T. Wallmersperger, *J. Intel. Mat. Syst. Str.* **2009**, *20*, 949.
[39] B. Barriere, L. Leibler, *J. Polym. Sci. Pol. Phys.* **2003**, *41*, 166.
[40] V. V. Yashin, O. Kuksenok, P. Dayal, A. C. Balazs, *Rep. Prog. Phys.* **2012**, *75*, 066601.
[41] P. Dayal, O. Kuksenok, A. C. Balazs, *Langmuir* **2009**, *25*, 4298.
[42] P. Dayal, O. Kuksenok, A. C. Balazs, *Soft Matter* **2010**, *6*, 768.
[43] P. Dayal, O. Kuksenok, A. C. Balazs, *Proc. Natl. Acad. Sci. USA* **2012**, DOI:10.1073/pnas.1213432110.